Vol. 56: 21–32, 2013
doi: 10.3354/cr01141

CLIMATE RESEARCH
Clim Res

Published February 21

Dynamic responses of soil organic carbon to climate change in the Three-River Headwater region of the Tibetan Plateau

Dongsheng Zhao[1,*], Shaohong Wu[1,2], Yunhe Yin[1]

[1]Institute of Geographical Sciences and Natural Resources Research, Chinese Academy of Sciences, 11A Datun Road, Anwai, Beijing 100101, PR China

[2]Institute of Tibetan Plateau Research, Chinese Academy of Sciences, 18 Shuangqing Road, Beijing 100085, PR China

ABSTRACT: Climate change has a high chance of stimulating soil organic carbon (SOC) decomposition, thereby accelerating carbon release in soil. Alpine ecosystems sequester large amounts of SOC. However, little is known about long-term trends and future changes of SOC in alpine ecosystems. In this study, the Lund-Potsdam-Jena dynamic global vegetation model for China (LPJ-CN) was applied to simulate temporal and spatial responses of soil organic carbon density (SOCD) to climate change in Three-River Headwater (TRH) of the Tibetan Plateau from 1981 to 2100. LPJ-CN is a modified dynamical vegetation model based on Chinese terrestrial ecosystem features. Results suggest that average SOCD for the TRH in the period from 1981 to 2010 was 3.97 kg C m^{-2}. During this period, SOCD increased at an average rate of 0.0001 kg C m^{-2} yr^{-1}; spatially there was a gradient of decreasing SOCD from east to west across the TRH. Under climate change scenarios, SOCD over TRH as a whole is projected to decrease until reaching it lowest level circa 2070, and to rise thereafter. However there may be some regional variation, with SOCD increasing in west TRH and decreasing in east TRH. This decreasing trend may be enhanced further in a warming climate. However, the pattern of higher SOCD in the east and lower SOCD in the west may have less variation in the future. In general, climate warming in the future may lead to a corresponding decrease in SOCD in TRH, which may accelerate carbon release from alpine soils.

KEY WORDS: Three-River Headwater · Soil organic carbon · Climate change · Dynamic responses · Tibetan Plateau

1. INTRODUCTION

The terrestrial ecosystem carbon (C) cycle is important for global climate change, since—according to the IPCC (2007)—global soil contains roughly 3 times the amount of C as that contained in vegetation and twice the amount as that in the atmosphere. Hence, minor changes in soil C stock will have significant effects on atmospheric CO_2 concentration (Johnston et al. 2004). Terrestrial ecosystems in high latitudes of the Northern Hemisphere are considered important C sinks because of their high soil organic carbon density (SOCD). A close correlation exists between the magnitude of C sinks and climate because C is sensitive to climate change. Climate change affects the sequestration and release of soil organic carbon (SOC). Changes in SOC stock will alter the atmospheric CO_2 content, which could either weaken or enhance the greenhouse effect. The Tibetan Plateau, also called the 'third pole' of the Earth, has a unique environment, diverse vegetation, and high climate-change sen-

*Email: zhaods@igsnrr.ac.cn

sitivity (Yao et al. 2000). A large amount of C could be sequestrated in the soil of the Tibetan Plateau for a long period because of its cold and relatively humid climate. However, climate change in the Tibetan Plateau is marked, with an average temperature increment of 0.36°C (10 yr)$^{-1}$ in the past 50 yr (Yi et al. 2011). Permafrost thawing has accelerated and soil microbial activities have been enhanced by this increase in temperature. Thus, the decomposition rate of SOC has also changed (Zhang et al. 2006, Li et al. 2009). Therefore, study of the estimated effect of future climate change on SOC in alpine ecosystems addresses an important issue in terrestrial carbon cycle research and can provide useful inputs for environmental policy making.

The SOC of alpine ecosystems elicited considerable research attention. SOC stock has been estimated in different soil types in the Tibetan Plateau using soil surveys (Wang et al. 2003). Yang et al. (2009) reported that SOC stock in alpine grasslands remained relatively stable from 1980 to 2004, based on a comparison of data from the Second National Soil Survey, completed in the early 1980s, and with more recent field soil sample data. Zhang et al. (2006) used century model simulation and found that SOC decomposition in alpine grasslands has accelerated over the past 40 yr because of climate change. The majority of global climate change models show that global warming will result in the loss of soil C (Sundquist 1993), particularly in high latitudes characterized by relatively low temperatures (Kirschbaum 1995). Oechel et al. (2000) reported that C sinks turn into a C source in northern high-latitude tundra ecosystems under climatic warming. Goulden et al. (1998) found that SOC is very sensitive to freezing depth and thawing time caused by global warming. Based on their research on the C balance of black spruce *Picea mariana* ecosystems in Canada they found that black spruce ecosystems could become a C source because of climate warming. Field experiments and observations of alpine ecosystems suggest that the soil of alpine ecosystems may release large amounts of C and become an atmospheric C source as the climate warms (Zhang et al. 2003, Xu et al. 2005, Zhao et al. 2005). However, little is known about long-term trends and future projected changes of SOC in alpine ecosystems.

Three-River Headwater (TRH) (Fig. 1), which is located in the southeast of the Tibetan Plateau, is the source of the Yangtze, Yellow, and Lanchang Rivers. the TRH covers approximately 3.63 × 10^5 km^2 with an average altitude of over 4000 m above mean sea level. The TRH has a plateau continental climate, where climate regimes switch from predominantly cold and dry to warm and dry. TRH vegetation mainly consists of alpine grassland, which accounts for more than 70 % of the total TRH area and contains the highest density of soil carbon on the Tibetan Plateau (Wang et al. 2010). The TRH is the main body of the Tibetan Plateau, where plant growth is heavily affected by specific climatic conditions, thus being sensitive to climate change, which makes it ideal for studies on the effects of climate change on ecosystems (Zhao 2009). In recent years, alpine ecosystem research for the TRH has attracted much attention, particularly after the implementation of Ecological Protection and Construction Project of TRH (EPCPTRH) by the Chinese central government in 2005 (Liu et al. 2010). The TRH has become a focal area for alpine ecosystem research. Therefore, the TRH was selected as the study area for this research.

Climate change affects sequestration and decomposition of SOC in 2 major ways: (1) through plant productivity and litter input rate, and (2) through decomposition rate of litter and SOC. It is likely that these 2 aspects interact and are inseparable from one another, whereas past studies that consider the 2 processes are still not yet conclusive (Johnston et al. 2004). A dynamic vegetation model based on biophysical, biogeographical and biogeochemical process

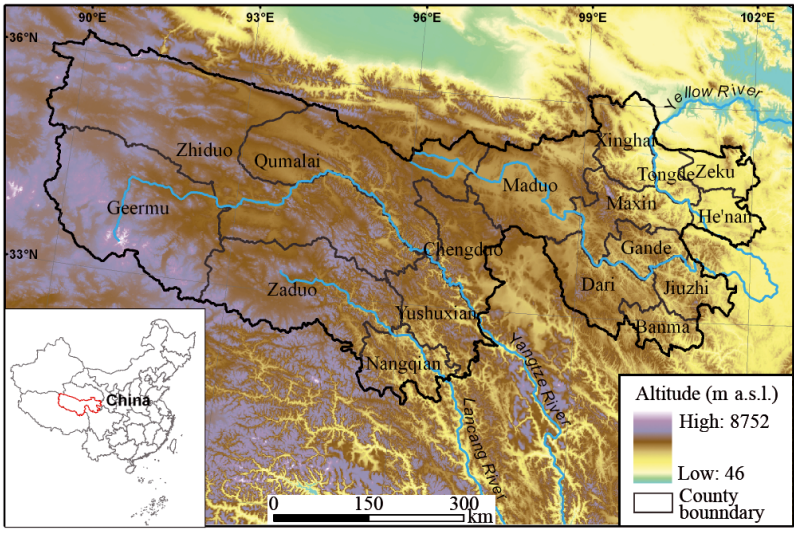

Fig. 1. Three-River Headwater on the Tibetan Plateau. Heights are given in metres above sea level

provides an effective approach to overcome these uncertainties. In this study, SOC dynamics in TRH was simulated with a modified Lund-Potsdam-Jena (LPJ) dynamic global vegetation model (DGVM) (Sitch et al. 2003, Gerten et al. 2004), which was calibrated to simulate ecosystem dynamics in China (Zhao et al. 2010). The study projects the future effects of climate change on SOC in TRH under 2 regional climate scenarios.

2. METHODS AND DATA

2.1. Methods

The LPJ model (Sitch et al. 2003, Gerten et al. 2004) is an intermediate complex DGVM, which was developed based on the early equilibrium model (BIOME3) and incorporates many features of BIOME series models. For example, the establishment and death of natural vegetation are mainly controlled by bioclimatic limits, and gross primary productivity of each functional type is calculated by the coupling of carbon and water. LPJ combines terrestrial vegetation dynamics and carbon and water exchanges in a modular framework. LPJ can also simulate carbon and nutrient cycling among plant-soil-atmosphere interfaces, as well as photosynthesis, net primary productivity (NPP), and carbon storage of vegetation and soil. In LPJ, litterfall from vegetation enters above and below ground litter pools. Part of the litter decomposes and transforms into CO_2, which is directly released into the atmosphere. The remaining litter is divided into slow and fast soil organic matter (SOM) pools. Decomposition rate (k) is a function of soil temperature and moisture. Temperature dependence $g(T)$ follows the modified Arrhenius relationship (Lloyd & Taylor 1994). The soil moisture relationship $f(w)$ is from Foley (1995). Decomposition rate, temperature dependence, and soil moisture relationship are expressed as:

$$k = \frac{(1/\tau_{10})g(T)f(w)}{12} \quad (1)$$

$$g(T) = \exp\left[308.56 \cdot \left(\frac{1}{56.02} - \frac{1}{(T+46.02)}\right)\right] \quad (2)$$

$$f(w) = 0.25 + 0.75 w_1 \quad (3)$$

$$c = c_0 \cdot e^{-kt} \quad (4)$$

where τ_{10} is the decomposition rate for SOM at 10°C, c is the pool size at time t with c_0 representing its initial size, T is the soil temperature, and w_1 is the average moisture status in the upper soil layer.

The semi-empirical approach of Haxeltine & Prentice (1996) is used to model soil hydrology with snowmelt, freeze/thaw, percolation, rainfall, evapotranspiration, and runoff considered. A detailed description on soil hydrology is given by Gerten et al. (2004).

Soil temperature follows surface temperatures with damped oscillation, which is the function of surface temperature and soil thermal diffusivity that depends on soil texture and soil water content. Soil temperature at depth z and time t is assumed to follow an annual sinusoidal cycle of air temperature (Campbell & Norman 2000).

$$T(z,T) = T_{ave} + A \cdot \exp(-z \cdot d^{-1}) \sin(\Omega \cdot \Delta t - z \cdot d^{-1}) \quad (5)$$

Here, T_{ave} represents the mean annual temperature above the respective layer, A represents amplitude of temperature fluctuation. $d = \sqrt{2k \cdot \Omega^{-1}}$ is the damping depth with thermal diffusivity $k = \lambda \cdot c^{-1}$, where c is the volumetric heat capacity and λ is the thermal conductivity. Ω is the angular frequency of oscillation.

LPJ replicates spatial permafrost distribution by using the normalized frost index F (Nelson & Outcalt 1987), which can be expressed as

$$F = \sqrt{D_f}\,(\sqrt{D_t} + \sqrt{D_f})^{-1} \quad (6)$$

where D_f represents annual freezing degree-days, and D_t represents the annual thawing degree-days.

Thaw depth represents soil depth z of the 0°C isotherm. Thaw depth is computed by applying Newton's method by finding the null of Eq. (5) numerically for each simulation day.

$$z_{n+1} = z_n + T(z_{n,t})(T'(z_{n,t}))^{-1} \quad (7)$$

where T' is the estimate of T. If a thawing or freezing event occurs, then associated soil water will shift between the separate pools for water and ice for each layer, and soil moisture is recalculated, which influences soil thermal properties for the next simulation day. See Sitch et al. (2003) and Gerten et al. (2004) for more detailed descriptions of LPJ.

Many characteristics of Chinese ecosystems are not reflected in LPJ because LPJ research has been mainly conducted in Europe and America. Therefore, in its original form, LPJ is not suitable in simulating ecosystem dynamics in China. In accordance with ecosystem characteristics in China, LPJ was modified by adding shrub and cold grass plant functional types (PFTs), updating PFT bioclimatic limits, and adopting the Penman-Monteith scheme to compute evapotranspiration. Simulation results of this modified LPJ-DGVM for China (LPJ-CN) were validated with observed datasets (Zhao et al. 2010). Simulation results of NPP from LPJ-CN match observed data

(R^2 = 0.64, p < 0.01), yielding better results than the original LPJ-DGVM (R^2 = 0.10) used by Ni (2003). Therefore, LPJ-CN is appropriate for simulating ecosystems in China. Details of LPJ-CN are given in Zhao et al. (2010). In the present study, LPJ-CN was employed to simulate responses of SOC to climate change.

2.2. Data

2.2.1. Climate baseline

Observed climatic data, including monthly mean temperature, monthly mean maximum temperature, monthly mean minimum temperature, monthly precipitation, monthly precipitation days, monthly mean relative humidity, monthly mean wind speed, and monthly sunshine hours, were obtained for 30 stations across the TRH and neighbouring areas from 1981 to 2010 from the National Climate Centre of the China Meteorological Administration. To obtain climatic grid data, station point data were interpolated to continuous surfaces with spatial resolutions of 0.1° × 0.1° latitude and longitude by using the thin plate spline method (Hutchinson 1998, Zhao et al. 2009). The observed climatic data from 1981 to 2010 were treated as the baseline condition for initial model calibration.

2.2.2. Climate scenarios

Climate scenarios in the late 21st century were produced by the Institute of Environment and Sustainable Development in Agriculture affiliated with the Chinese Academy of Agricultural Sciences using the Providing Regional Climate for Impacts Studies (PRECIS) system (Jones et al. 2004) based on the IPCC's 'Special Report on Emission Scenarios' (Nakicenovic et al. 2000). These climate scenarios have been widely applied in various assessments of climate change in China (Xiong et al. 2009, Wu et al. 2010, H. Yang et al. 2010, Zhao et al. 2011). In this study, the climatic data for A2 and B2 scenarios were selected to evaluate the effects of climate change on SOCD on TRH. The A2 scenario has higher emissions of greenhouse gases and is characterized by self-reliance, local identities, and continuous population growth. Economic development is regionally oriented. The B2 scenario represents moderate emissions of greenhouse gases and is characterized by a continued but moderated increase in population and moderate economic growth, with emphasis on local solutions for economic, social, and environmental sustainability. We calculated monthly mean anomalies from the difference between observed data and PRECIS-generated data for the baseline term (1981 to 2010), and then added the anomalies to scenario data to provide model input for the scenario period (2011 to 2100).

Following PRECIS, annual mean temperature in the TRH (Fig. 2) is projected to increase by 4.1°C under A2 and by 2.6°C under B2 compared with the average annual mean temperature from 1981 to 2010. The magnitude of the temperature increase

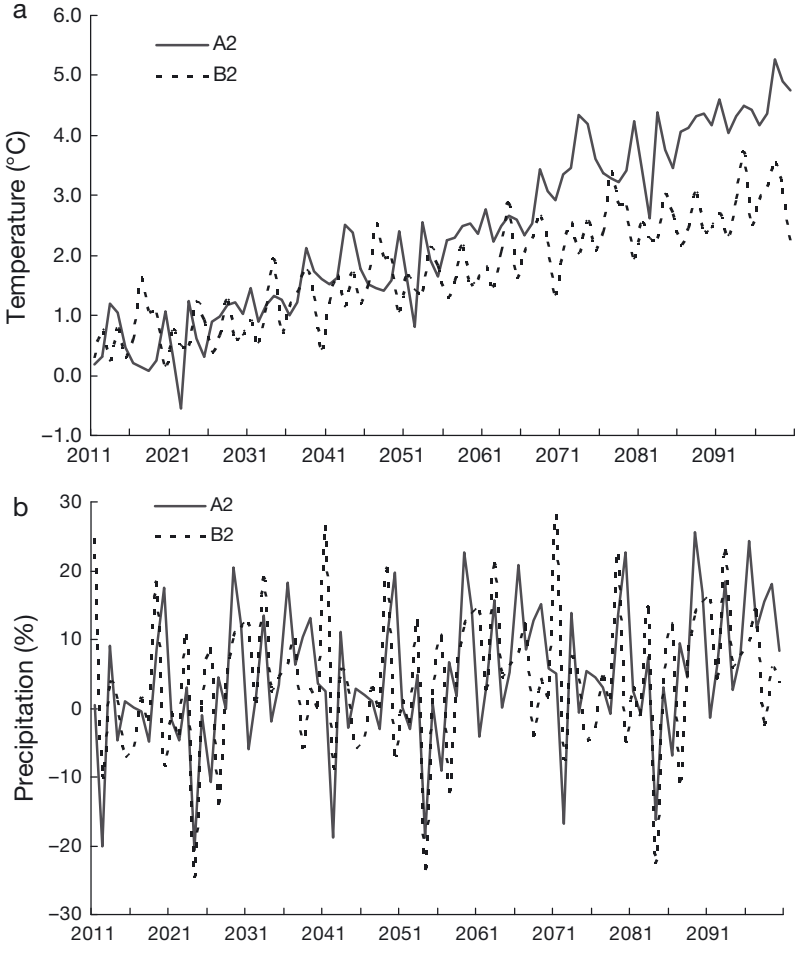

Fig. 2. Variations of (a) temperature (°C) and (b) precipitation (%) in Three-River Headwater under the A2 and B2 climate change scenarios from IPCC's 'Special Report on Emission Scenarios' (Nakicenovic et al. 2000) relative to the averages of the baseline period 1981–2000

reduces from southwest to northeast of the TRH, with the largest increase occurring in Henan and Jiuzhi. Total annual precipitation is projected to increase by 6 to 7% (B2). The highest increase in total annual precipitation occurs at the middle part of the TRH, including Chengduo, Maduo, and Yushuxian. Slight decreases in precipitation occur in Nanqian and Zhiduo.

This study utilized four 30 yr periods to study spatial and temporal variations in SOCD: the baseline period 1981 to 2010; near term: 2011 to 2040; mid term: 2041 to 2070; and long term: 2071 to 2100.

2.2.3. Soil data

Soil-texture data from the map of soil texture types (1:14 000 000) (Zhang et al. 2004) was used in this study. Soil-texture data provided information on the proportions of mineral grains of different sizes in topsoil and the geographical distribution of different soil texture types in a given region. The soil textures were classified as clay, silt, sand, silty sand, sandy clay, silty clay, and clay with silt and sand following the standard classification of soil texture of the Food and Agriculture Organization of the United Nations (Ni et al. 2000) to meet model input requirements. Soil data were then transformed into ArcInfo9.3 grid format and resampled to a spatial resolution of 0.1 × 0.1° latitude and longitude.

2.2.4. Measured SOCD data

Observed SOCD data were obtained from Y. H. Yang et al. (2010), who produced an SOCD dataset on the grasslands of northern China. The SOCD dataset contained soil data derived from the National Soil Inventory of China produced during the 1980s and 5 consecutive annual regional soil surveys on the grasslands of China from 2001 to 2005. The inventory recorded geographic location, land cover information, layer thickness, bulk density, and SOM. SOM was converted to SOC using the constant 0.58 (Xie et al. 2007). In the 5 consecutive soil surveys, 327 sites were sampled across the grasslands of northern China. At each site, 3 profiles were taken at depths of 0–10, 10–20, 20–30, 30–50, 50–70, and 70–100 cm. SOC concentration was analyzed with Walkley-Black method (Nelson & Sommers 1982) after soil samples were sieved through a 2 mm mesh and ground in a ball mill. The part of this dataset corresponding to TRH was extracted for use in this study.

3. RESULTS

3.1. Validation of simulated SOCD and its inter-annual change in the period 1981–2010

SOCD simulated by LPJ-CN was closely correlated with actual measurements ($R^2 = 0.62$), thus indicating that LPJ-CN is reliable for regional SOCD assessment (Fig. 3). The average SOCD simulated across the TRH in the period 1981–2010 was 3.97 kg C m^{-2}. The annual average of simulated SOCD increased

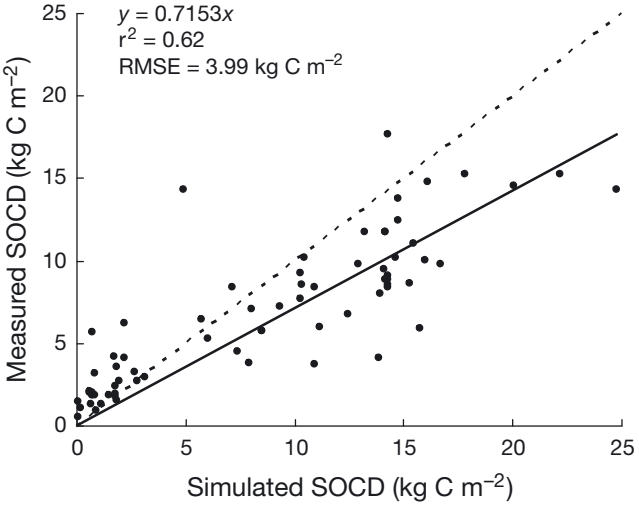

Fig. 3. Comparison between simulated and measured soil organic carbon density (SOCD) in Three-River Headwater in the baseline period 1981–2010

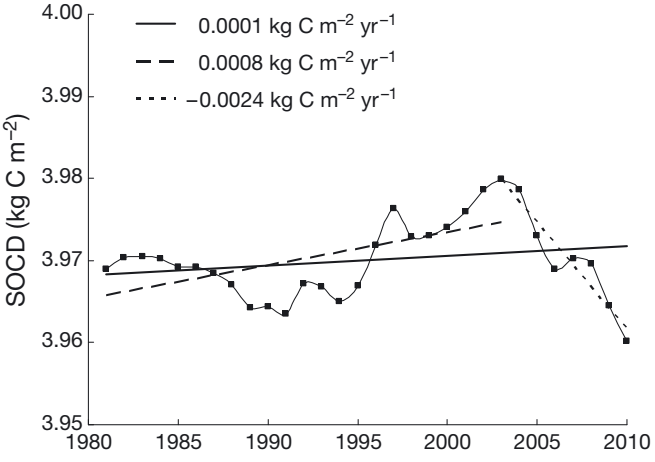

Fig. 4. Inter-annual variation of soil organic carbon density (SOCD) in Three-River Headwater from 1981 to 2010, showing trend lines and average changes for the periods 1981–2010 (solid line), 1981–2003 (long-dashed line) and 2003–2010 (short-dashed line)

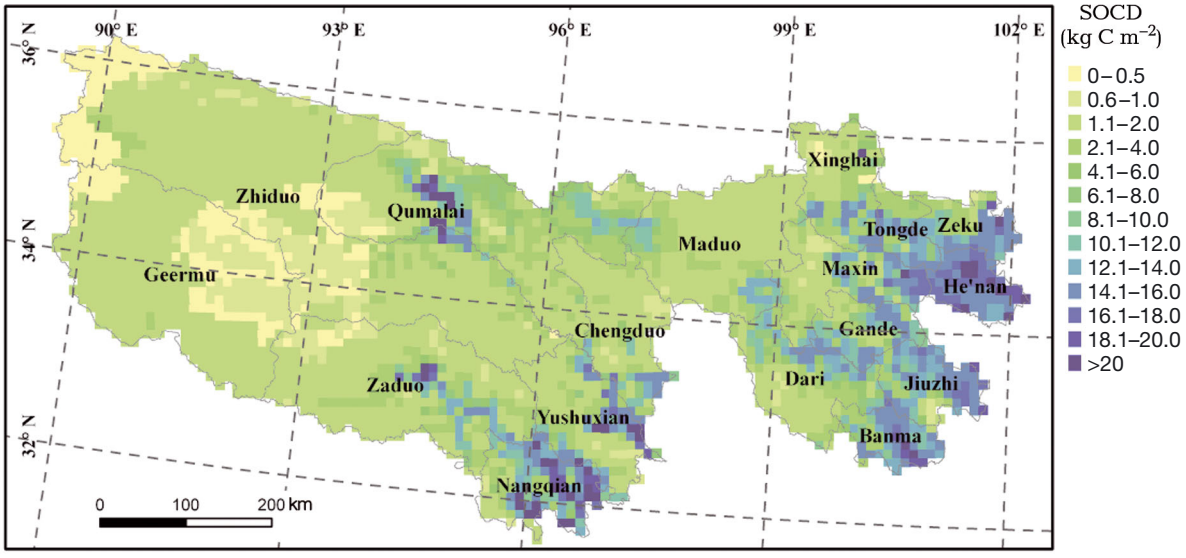

Fig. 5. Spatial variation of average soil organic carbon density (SOCD) in Three-River Headwater from 1981 to 2010

by 0.0001 kg C m^{-2} yr^{-1}. Although a statistically significant trend of SOCD was found from 1981 to 2010 (R^2 = 0.1, $p < 0.001$), there were 2 distinct periods, with opposite trends before and after 2003 (Fig. 4). SOCD, spatially averaged over the TRH, increased by 0.0008 kg C m^{-2} yr^{-1} from 1981 to 2003 (R^2 = 0.36, $p < 0.05$), and decreased by 0.0024 kg C m^{-2} yr^{-1} (R^2 = 0.92, $p < 0.001$) from 2003 to 2010. SOCD values decreased from the east to the west of the TRH, with higher SOCD values (>10 kg C m^{-2}) in Nangqian, Banma, Jiuzhi, and Henan, and lower ones (<0.5 kg C m^{-2}) in west Zhiduo and Tanggulaxiang affiliated Geermu (Fig. 5).

3.2. Changes in SOCD at the regional scale in the future

Fig. 6 illustrates the inter-annual variation in SOCD in the future at a regional scale. SOCD shows remarkable decreasing trends of –0.0016 kg C m^{-2} yr^{-1} (R^2 = 0.60, $p < 0.001$) and –0.0017 kg C m^{-2} yr^{-1} (R^2 = 0.76, $p < 0.001$) under A2 and B2 scenarios, respectively. However, 2070 appears to be a turning point for SOCD. Two periods with opposite trends can be distinguished before and after 2070. During the period 2011 to 2070, SOCD declines at –0.0032 kg C m^{-2} yr^{-1} (R^2 = 0.95, $p < 0.001$) and –0.0029 kg C m^{-2}

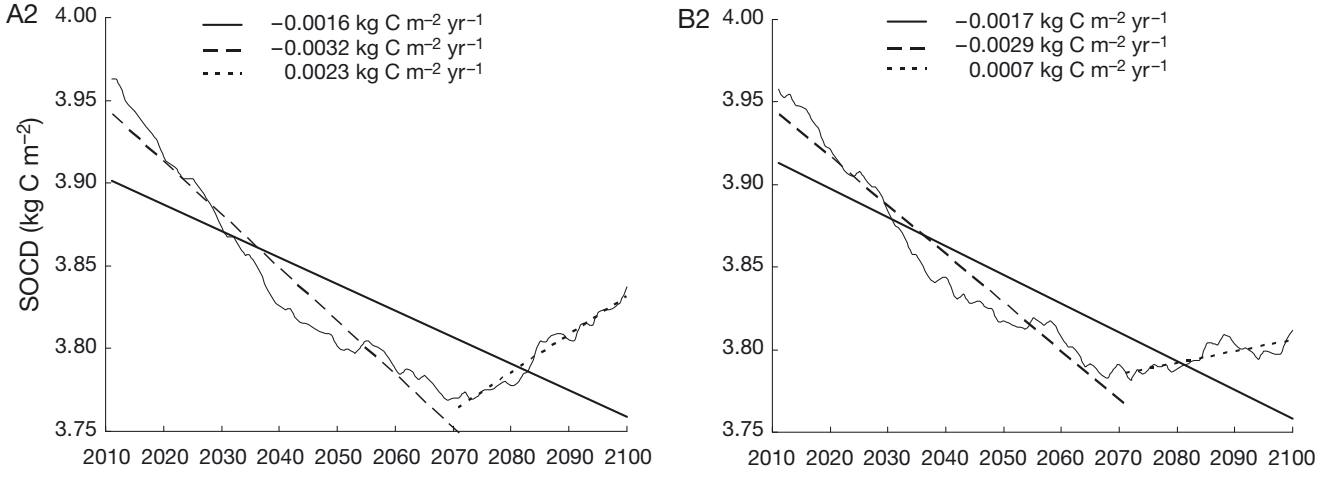

Fig. 6. Inter-annual variation of soil organic carbon density (SOCD) in Three-River Headwater from 2011 to 2100 under A2 (left) and B2 (right) scenarios, showing trend lines and average changes for the periods 2011–2100 (solid line), 2011–2070 (long-dashed line) and 2071–2100 (short-dashed line)

yr^{-1} (R^2 = 0.95, p < 0.001) under A2 and B2 scenarios, respectively. Minimum SOCD is approximately 94% of the average level in the baseline period. After 2071, SOCD shows rising trends in both scenarios, i.e. 0.0023 kg C m^{-2} yr^{-1} (R^2 = 0.96, p < 0.001) under A2, and 0.0007 kg C m^2 yr^{-1} (R^2 = 0.61, p < 0.001) under B2.

3.3. Spatial patterns of SOCD during different warming periods

The spatial pattern of SOCD in the near term (Fig. 7) is similar to that in the baseline period. SOCD decreases over most areas of the TRH (64 and 60% of the study area under A2 and B2 scenarios, respectively). The average decrement in SOCD is ~0.15 kg C m^{-2} compared to the baseline period. The most pronounced decrease in the near term (>0.7 kg C m^{-2}) occurs in the south and east of the TRH. The west of the TRH experiences a slight increase (<0.1 kg C m^{-2}).

No obvious spatial changes of SOCD occur in the mid term compared with the near term, but the magnitude of variation in SOCD intensifies in the mid-term period (Fig. 8). SOCD shows an increasing trend in 58% (A2) and 41% (B2) of the study area. Average increments in SOCD are projected to be 0.39 and 0.59 kg C m^{-2} under A2 and B2 scenarios,

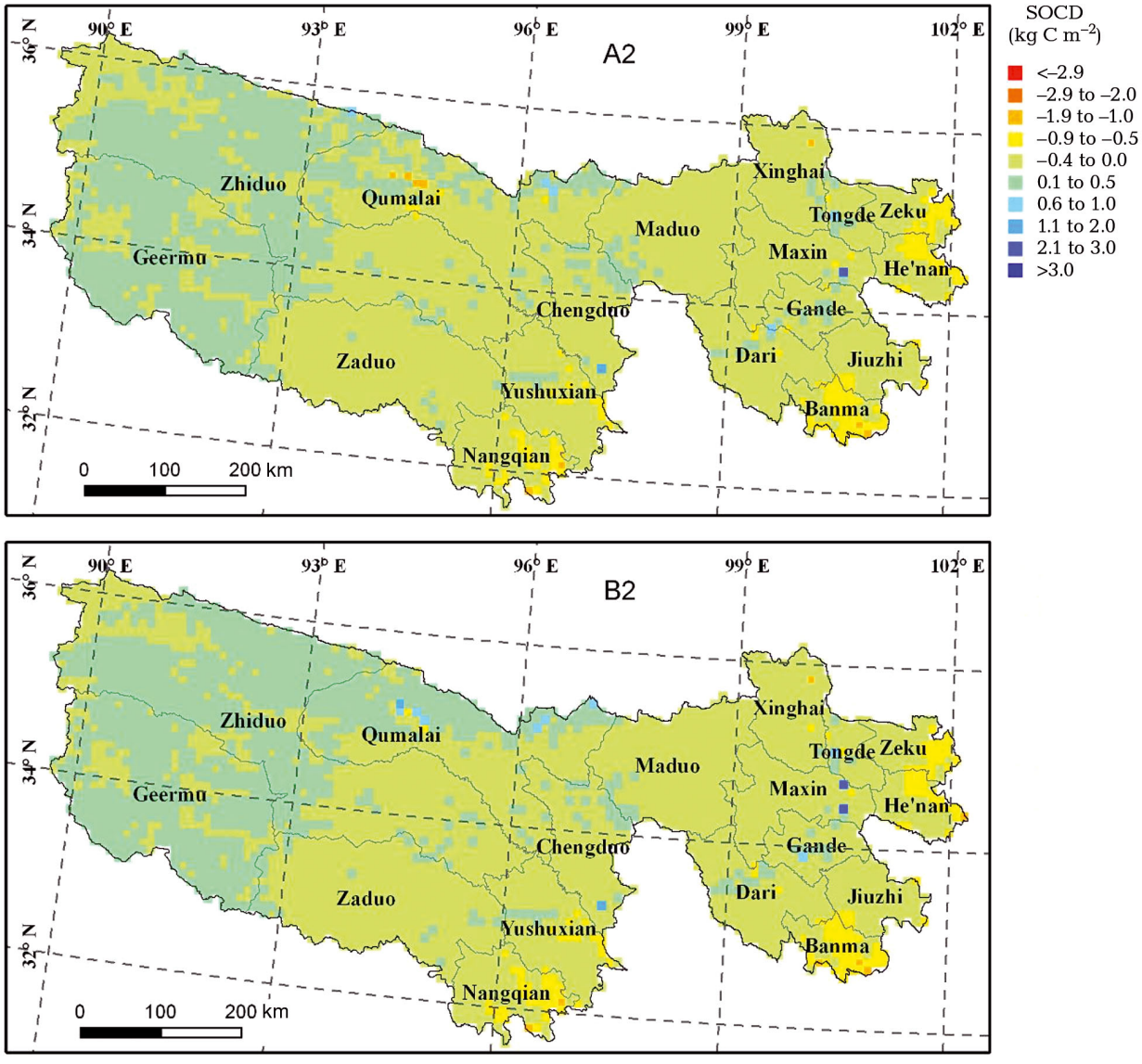

Fig. 7. Spatial variation of changes in soil organic carbon density (SOCD) in the near term (2011–2040), compared with the baseline period 1980–2010, under A2 (top) and B2 (bottom) scenarios

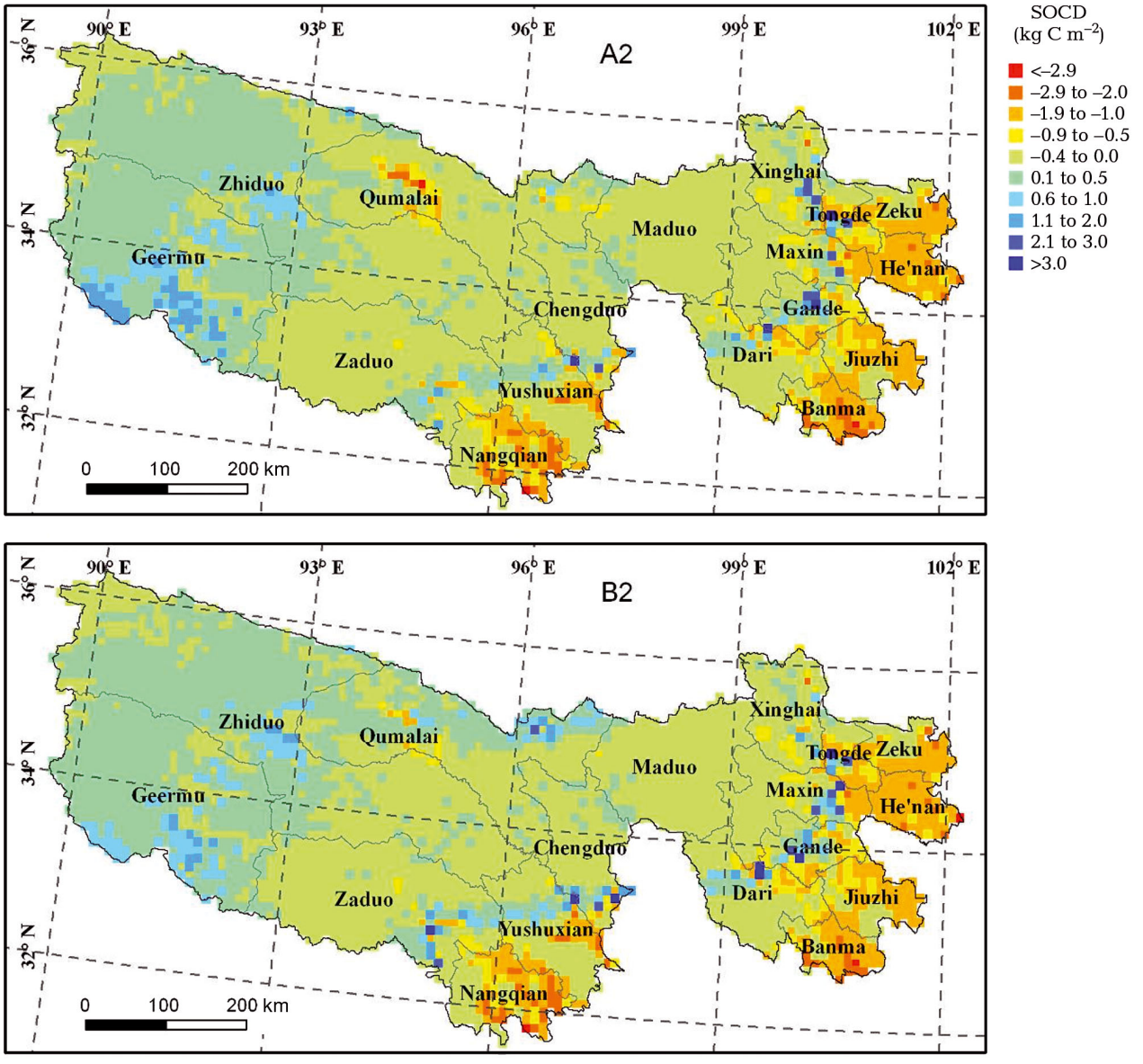

Fig. 8. Spatial variation of changes in soil organic carbon density (SOCD) in the mid term (2041–2070), compared with the baseline period 1980–2010, under A2 (top) and B2 (bottom) scenarios

respectively. The largest decrements (>1 kg C m^{-2}) occur in the east and south of TRH, principally in Henan, Banma, Dari, and Nanqian. SOCD increases by 0.25 kg C m^{-2} in the west of TRH.

A slight expansion in the area of SOCD showing a decreasing trend occurs in the long term (Fig. 9), when it accounts for 58% (A2) and 59% (B2) of the total TRH area. However, the magnitude of the decrement in SOCD is greater, i.e. approximately 0.76 and 0.67 kg C m^{-2} under A2 and B2 scenarios respectively. The greatest decrements still exist in 4 counties of the east and south as that in the mid term simulation; however, the magnitude of the decrement in SOCD (> 3 kg C m^{-2}) is far higher than that in the mid term. SOCD in the west of the TRH is likely to keep increasing, and the range of values across the region is projected to increase compared with the mid term, particularly for the A2 scenario.

4. DISCUSSION

Simulated average SOCD from 1981 to 2010 in LPJ-CN is close to calculation of Y. H. Yang et al.

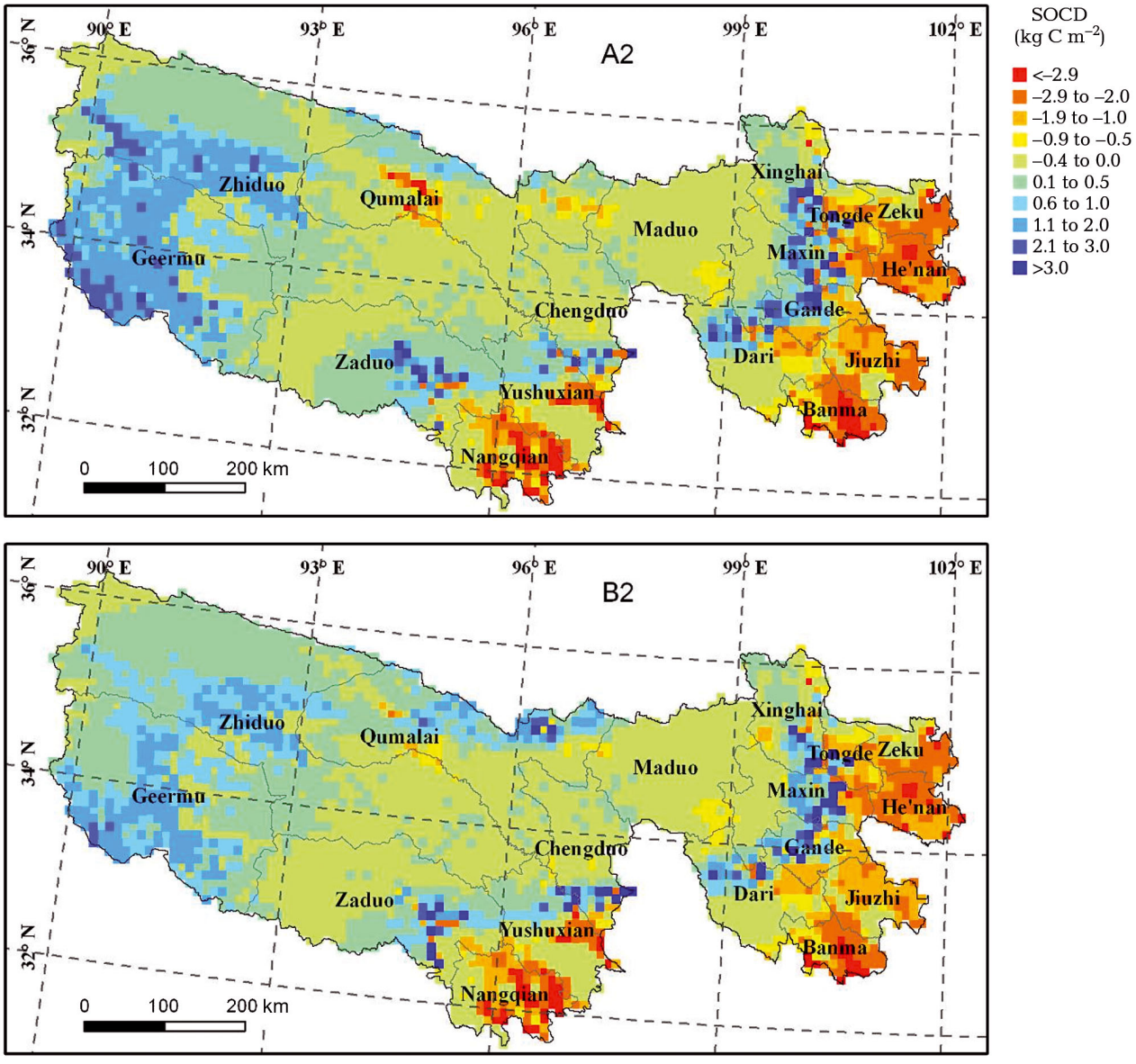

Fig. 9. Spatial variation of changes in soil organic carbon density (SOCD) in the long term (2071–2100), compared with the baseline period 1980–2010, under A2 (top) and B2 (bottom) scenarios

(2010) (3.9 kg C m^{-2}) based on soil inventory and field soil survey data. Although the results of Y. H. Yang et al. (2010) apply only to grasslands, comparing the 2 studies is reasonable because grasslands occupy more than 70% of the total area of TRH. The spatial pattern of SOCD, decreasing from southeast to northwest of TRH, found in this study is similar to that found by Xie et al. (2004) and Wang et al. (2003) using a comprehensive soil survey. Based on these comparisons, LPJ-CN can be considered to capture the basic dynamics of regional SOCD in TRH.

SOCD in the TRH shows significant inter-annual change from 1981 to 2010, but the trend was not consistent over the 30 yr period. The maximum change in SOCD compared to the average in the baseline period was –2.5% in 2003. The opposing trends found before and after 2003 indicate that variations in SOCD are sensitive to climate change in the TRH. The decreasing trend in SOCD after 2003 is associated with rising temperature and increasing spatial heterogeneity of precipitation in the TRH. After 2003, decreasing precipitation in the east tended to result in SOC decomposition, but in con-

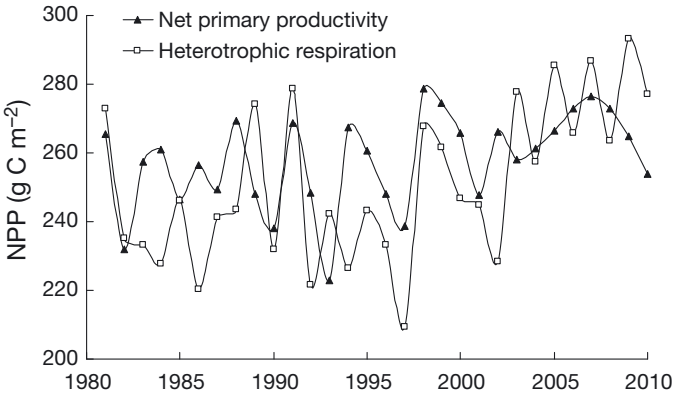

Fig. 10. Interannual variation of net primary productivity (NPP) and heterotrophic respiration in Three-River Headwater from 1981 to 2010

trast increasing precipitation in the west can induce SOC immobility. While SOCD showed a declining trend in the TRH as a whole after 2003, heterotrophic respiration across the TRH showed a significant increasing trend, with an increase higher than that for NPP (Fig. 10). Y. H. Yang et al. (2010) reported that SOC in northern China's grassland remained relatively constant from the 1980s to the 2000s based on data from a soil field survey, since SOC dynamics of between 6% loss and 9% gain could not be detected by site-level comparison. Measuring C stock changes in the field by using direct measurements is a difficult task (Conen et al. 2003, Smith 2004). Simulation using ecosystem models is a very effective approach for detecting the effect of climate change on SOCD.

Under climate change scenarios A2 and B2, SOCD in TRH shows a significant declining trend in the period after 2010. Climate change in the future is likely to be characterized by rising temperature and slightly increasing precipitation in this region (Fig. 2). These characteristics may stimulate plant production, by reducing low temperature limitation on plant growth and may accelerate microbial metabolism of SOM associated with heterotrophic respiration. Heterotrophic respiration will increase in the TRH because of the warming climate and is likely to be greater than plant production between 2011 and 2070, thus leading to the release of SOC. However the declining tendency of SOCD is reversed after 2071, particularly in the west, because of an NPP increment higher than that for heterotrophic respiration (Fig. 11).

Regional differences are apparent in the simulated responses of SOC to climate changes. SOCD tends to decrease in the east and increase in the west. This phenomenon may be caused by the regional difference in carbon inputs from plant production, which are likely to rise in the western region, but remain relatively constant or even decline in the eastern region. Based on observed data, Y. H. Yang et al. (2010) found that SOCD changes tend to be greater in areas with higher SOCD. Similarly, Holmes et al. (2006) showed that the direction of SOC change following forest clearing was related to original forest soil carbon content.

In this study, SOCD changes for the TRS in the 21st century remain uncertain because of limitations with regard to research methods. After parameters were modified and cold grass PFT were added in the original LPJ based on local ecosystem characteristics, the resulting LPJ-CN was able to capture the temporal and spatial pattern of SOC more effectively than the original LPJ model. Unlike some biogeochemical models that explicitly simulate fluxes of carbon and nitrogen for terrestrial ecosystem, LPJ has simplified algorithms for biogeochemical processes

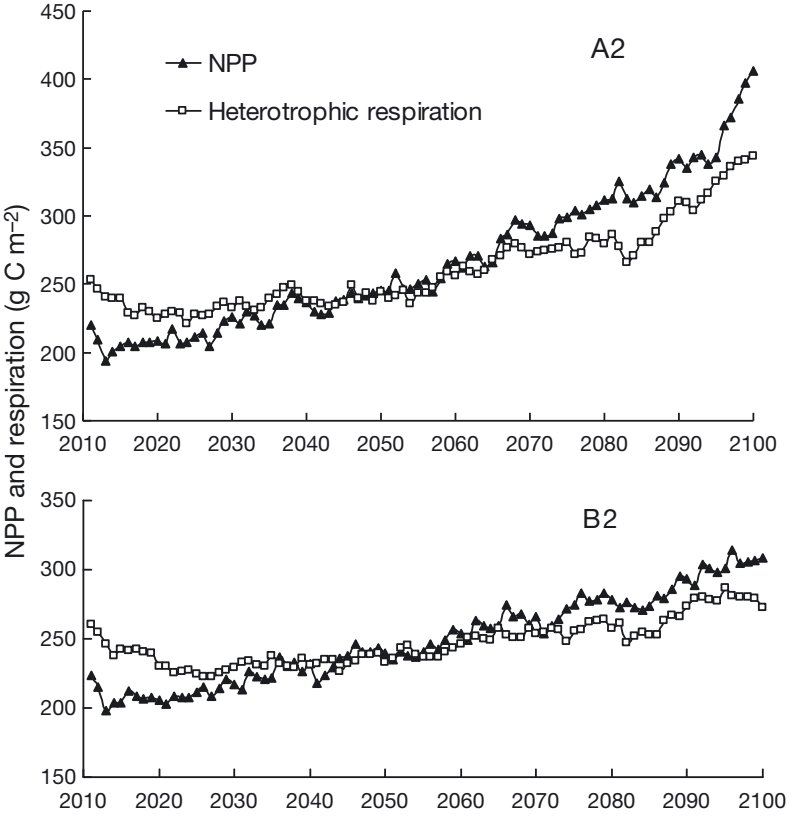

Fig. 11. Inter-annual variation of net primary productivity (NPP) and heterotrophic respiration in Three-River Headwater from 2011 to 2100 under A2 (top) and B2 (bottom) scenarios

to improve computational efficiency. For example, LPJ assumes that no limitations in nitrogen, phosphorus, and sulphur occur. However, SOC accumulation may be constrained by nitrogen (Hungate et al. 2003). Therefore, further work on parameter calibration and model improvement remains necessary.

In addition, the use of climate scenarios could lead to uncertainty of simulated results. General circulation models operating on resolutions of 200 to 300 km are coarse for studies of climate change effects on ecosystems at a regional scale. Although the output of PRECIS has been improved by enhancing spatial resolution in this study, such problems cannot be entirely eradicated to rule out uncertainties.

Finally, temporal and spatial changes of SOCD have been projected based on natural vegetation, which is free from the influence of human activities. The Tibetan Plateau is the largest and highest region in the world and has few residents. The TRH is among the most sparsely populated areas in the Tibetan Plateau. Moreover, the number of residents may fall further in the future because of enforced ecological migration associated with EPCPTRH, which will further reduce levels of human disturbance in the TRH.

Acknowledgements. This study was financially supported by the National Basic Research Program of China (2011 CB403206), National Natural Science Foundation of China (40901058), Commonweal Research Funding from the Ministry of Environmental Protection of China (201009056) and the National Scientific Technical Supporting Programs during the 11th Five-year Plan of China (2009BAC61B05). The authors thank Prof. Yinlong Xu from the Institute of Environment and Sustainable Development in Agriculture, Chinese Academy of Agriculture Sciences, for providing climate scenario data. We also appreciate 2 reviewers for their helpful comments and suggestions on an earlier version of manuscript.

LITERATURE CITED

Campbell GS, Norman JM (2000) An introduction to environmental biophysics, 2nd edn. Springer, New York

Conen F, Yakutin MV, Sambuu AD (2003) Potential for detecting changes in soil organic carbon concentrations resulting from climate change. Glob Change Biol 9:1515–1520

Foley JA (1995) An equilibrium model of the terrestrial carbon budget. Tellus 47B:310–319

Gerten D, Schaphoff S, Haberlandt U, Lucht W, Sitch S (2004) Terrestrial vegetation and water balance—hydrological evaluation of a dynamic global vegetation model. J Hydrol (Amst) 286:249–270

Goulden ML, Wofsy SC, Harden JW, Trumbore SE and others (1998) Sensitivity of boreal forest carbon balance to soil thaw. Science 279:214–217

Haxeltine A, Prentice I (1996) BIOME3: an equilibrium terrestrial biosphere model based on ecophysiological constraints, resource availability, and competition among plant functional types. Global Biogeochem Cycles 10:693–709

Holmes KW, Chadwick OA, Kyriakidis PC, Silva de Filho EP, Soares JV, Roberts DA (2006) Large-area spatially explicit estimates of tropical soil carbon stocks and response to land-cover change. Global Biogeochem Cycles 20:GB3004, doi:10.1029/2005GB002507

Hungate BA, Dukes JS, Shaw MR, Luo Y, Field CB (2003) Nitrogen and climate change. Science 302:1512–1513

Hutchinson MF (1998) Interpolation of rainfall data with thin plate smoothing splines. I. Two dimensional smoothing of data with short range correlation. J Geogr Inf Decis Anal 2:152–167

IPCC (2007) Climate change 2007: the physical science basis. Contribution of Working Group I to the Fourth Assessment Report of the Intergovernmental Panel on Climate Change. Cambridge University Press, Cambridge

Johnston CA, Groffman P, Breshears DD, Cardon ZG and others (2004) Carbon cycling in soil. Front Ecol Environ 2:522–528

Jones R, Noguer M, Hassell D, Hudson D, Wilson S, Jenkins G, Mitchell J (2004) Generating high resolution climate change scenarios using PRECIS. Met Office Hadley Centre, Exeter

Kirschbaum MUF (1995) The temperature dependence of soil organic matter decomposition and the effect of global warming on soil organic C storage. Soil Biol Biochem 27:753–760

Li N, Wang GX, Gao YH, Ji CZ (2009) On soil organic carbon of alpine ecosystem in Qinghai-Tibet Plateau. Soils 41:512–519 (in Chinese)

Liu XD, Liu RT, Liu AJ, Yun XJ, Li XY, Bao HM (2010) Study on information extraction and the dynamic monitoring of grassland coverage in Three River Source area. Acta Agrestia Sin 19:154–159 (in Chinese)

Lloyd J, Taylor JA (1994) On the temperature dependence of soil respiration. Funct Ecol 8:315–323

Nakicenovic N, Alcamo J, Davis G, de Vries B and others (2000) Special report on emissions scenarios: a special report of Working Group III of the Intergovernmental Panel on Climate Change. Cambridge University Press, Cambridge

Nelson FE, Outcalt SI (1987) A computational method for prediction and regionalization of permafrost. Arct Alp Res 19:279–288

Nelson DW, Sommers LE (1982) Total carbon, organic carbon, organic matter. In: Page AL (ed) Methods of soil analysis, Part 2 (2nd edn). American Society of Agronomy, Madison, WI, p 539–580

Ni J (2003) Net primary productivity in forests of China: scaling-up of national inventory data and comparison with model predictions. For Ecol Manag 176:485–495

Ni J, Sykes MT, Prentice IC, Cramer W (2000) Modeling the vegetation of China using the process-based equilibrium terrestrial biosphere model Biome3. Glob Ecol Biogeogr 9:463–479

Oechel WC, Vourlitis GL, Hastings SJ, Zulueta RC, Hinzman L, Kane D (2000) Acclimation of ecosystem CO_2 exchange in the Alaskan Arctic in response to decadal climate warming. Nature 406:978–981

Sitch S, Smith B, Prentice IC, Arneth A and others (2003) Evaluation of ecosystem dynamics, plant geography, and terrestrial carbon cycling in the LPJ dynamic global

vegetation model. Glob Change Biol 9:161–185
Smith P (2004) How long before a change in soil organic carbon can be detected? Glob Change Biol 10:1878–1883
Sundquist ET (1993) The global carbon dioxide budget. Science 259:934–941
Wang SQ, Tian HQ, Liu JY, Pan SF (2003) Pattern and change of soil organic carbon storage in China: 1960s–1980s. Tellus B 55:416–427
Wang GX, Cheng GD, Shen YP (2010) Soil organic carbon pool of grasslands on the Tibetan Plateau and its global implication. J Glaciol Geocryol 24:693–700 (in Chinese)
Wu SH, Yin YH, Zhao DS, Huang M, Shao XM, Dai EF (2010) Impact of future climate change on terrestrial ecosystems in China. Int J Climatol 30:866–873
Xie XL, Sun B, Zhou HZ, Li PZ (2004) Soil carbon stocks and their influencing factors under native vegetations in China. Acta Pedol Sin 41:687–698 (in Chinese)
Xie ZB, Zhu JG, Liu G, Cardisch G and others (2007) Soil organic carbon stocks in China and changes from 1980s to 2000s. Glob Change Biol 13:1989–2007
Xiong W, Conway D, Lin ED, Holman I (2009) Potential impacts of climate change and climate variability on China's rice yield and production. Clim Res 40:23–35
Xu LL, Zhang XZ, Shi PL, Yu GR, Sun XM (2005) Net ecosystem carbon dioxide exchange of alpine meadow on the Tibetan Plateau from August to October. Acta Ecol Sin 25:1948–1952 (in Chinese)
Yang H, Xu Y, Zhang L, Pan J, Li X (2010) Projected change in heat waves over China using the PRECIS climate model. Clim Res 42:79–88
Yang YH, Fang JY, Smith P, Tang YH and others (2009) Change in topsoil carbon stock in the Tibetan grasslands between the 1980s and 2004. Glob Change Biol 15: 2723–2729
Yang YH, Fang JY, Ma WH, Smith P, Mohammat A, Wang SP, Wang W (2010) Soil carbon stock and its changes in northern China's grassland from 1980s to 2000s. Glob Change Biol 16:3036–3047
Yao TD, Liu XD, Wang NL (2000) Amplitude of climatic changes in Qinghai-Tibetan Plateau. Chin Sci Bull 45: 1236–1243 (in Chinese)
Yi XS, Yin YY, Li GS, Peng JT (2011) Temperature variation in recent 50 years in the Three-River Headwaters region of Qinghai Province. Acta Geogr Sin 66:1451–1465 (in Chinese)
Zhang JX, Cao GM, Zhou DW, Hu QW, Zhao XQ (2003) The carbon storage and carbon cycle among the atmosphere, soil, vegetation and animal in the *Kobresia humilis* alpine meadow ecosystem. Acta Ecol Sin 23: 627–634 (in Chinese)
Zhang SH, Peng GB, Huang M (2004) The feature extraction and data fusion of regional soil textures based on GIS techniques. Clim Environ Res 6:65–79 (in Chinese)
Zhang YQ, Tang YH, Jiang J (2006) The dynamic characteristics of soil organic carbon on grassland in Qinghai-Tibetan Plateau. Sci China Ser D 12:1140–1147 (in Chinese)
Zhao DS, Wu SH, Zheng D, Yang QY (2009) Spatial pattern of eco-climatic factors on Tibetan Plateau. Chinese J Appl Ecol 20:1153–1159 (in Chinese)
Zhao DS, Wu SH, Yin YH (2010) Variation trends of natural vegetation net primary productivity in China under climate change scenario. Chinese J Appl Ecol 22:897–904 (in Chinese)
Zhao DS, Wu SH, Yin YH, Yin ZY (2011) Vegetation distribution on Tibetan Plateau under climate change scenario. Reg Environ Change 11:905–915
Zhao L, Li YN, Zhao XQ, Xu SX and others (2005) The comparative study of net ecosystem CO_2 exchanges of 3 typical vegetation types on the Qinghai-Tibetan Plateau. Chin Sci Bull 50:926–932 (in Chinese)
Zhao XQ (2009) Impacts of global change on alpine meadow ecosystem and related strategies. In Zhao XQ (ed) Alpine meadow ecosystem and global change. Science Press, Beijing, p 309–335 (in Chinese)

Editorial responsibility: Gouyu Ren, Beijing, China

Submitted: April 24, 2012; Accepted: October 25, 2012
Proofs received from author(s): January 31, 2013